2026 SCEC Annual Report

Determination of Shallow Crustal Structure in Northern California, the Bay Area, and Community Model Validation Using Rayleigh Wave Ellipticity, Receiver Functions, and Gravity

Report for SCEC Award 25266

PIs: Dr. Fan-Chi Lin
Department of Geology and Geophysics,
University of Utah, 115 S. 1460 E. Rm. 205,
Salt Lake City, UT 84112-0111

Dr. Taka'aki Taira
UC Berkeley Seismology Laboratory,
307 McCone Hall #4760 Berkeley, CA
94720-4760

Publications and Reports: None

Summary. This project aims to validate the shallow crustal structure of the USGS San Francisco Bay Area (SFBA) Community Velocity Model (CVM; Aagaard & Hirakawa, 2021) using Rayleigh-wave ellipticity (horizontal-to-vertical, H/V, amplitude ratios) and receiver functions. To this end, we compute multi-component ambient noise cross-correlations from stations in the NC, BK, and NP networks across Northern California. Rayleigh-wave signals in the 3–10 s period range are extracted to measure station- and period-dependent H/V ratios. We compare the observed H/V ratios with predictions from the SFBA CVM. While the two exhibit broadly similar patterns, notable discrepancies are present in several regions. In particular, higher observed H/V ratios in the Oakland and San Jose areas adjacent to the South Bay suggest inconsistencies between the SFBA CVM and the true shallow sedimentary structure. We invert the H/V ratios to derive new 1D shallow crustal models across SFBA. These models have been compared with SFBA CVM in this report and used to evaluate earthquake ground-motion predictions in a separate study (see the project report of SCEC Award 25296). Efforts to incorporate receiver functions into the validation and inversion are ongoing.

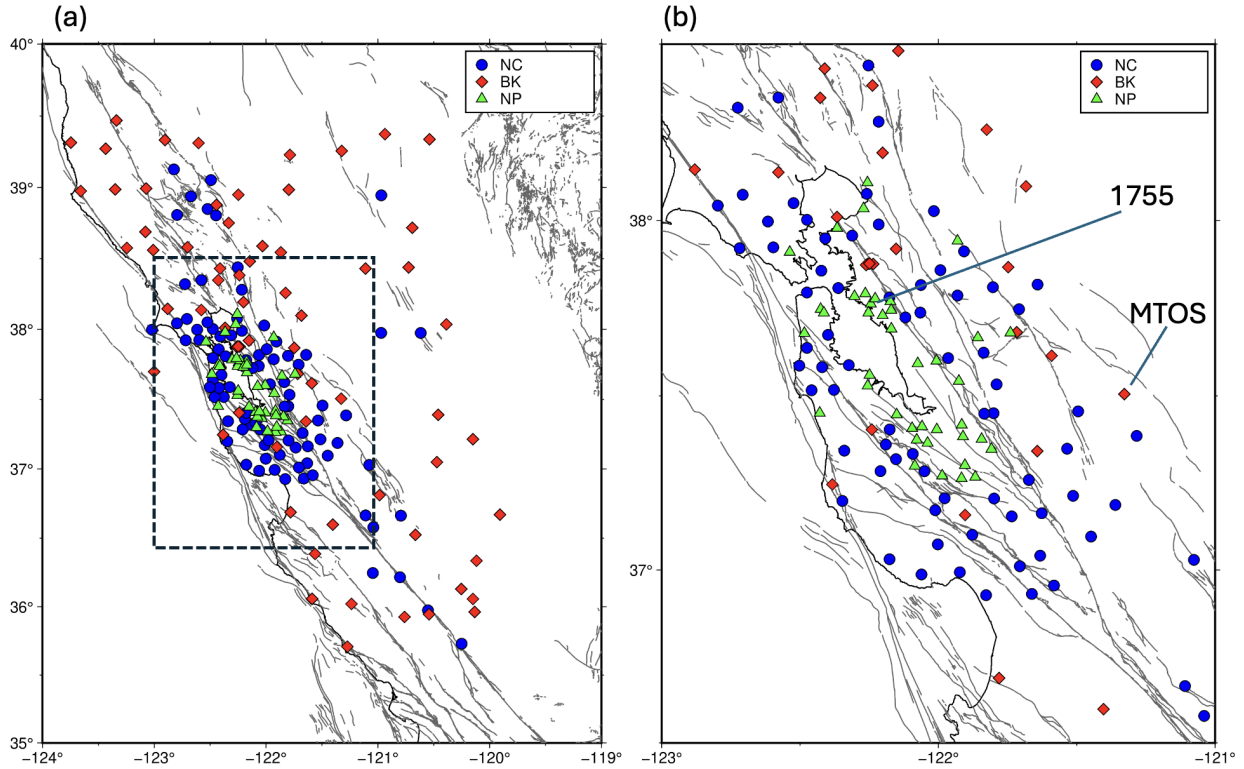

Figure 1. Station map. (a) Locations of NC, BK, and NP stations used in this study. The dashed box outlines the San Francisco Bay Area (SFBA), shown in (b). (b) Same as (a), but zoomed in on the SFBA. The MTOS and 1755 stations used in the later figures are identified.

Multi-Component Ambient Noise Cross-Correlation

We perform multi-component noise cross-correlations following the method described in Lin et al. (2014). Three-component ambient noise data recorded by available NC, BK, and NP network stations between January 1 and March 31, 2025, are used in the analysis. For each station, temporal and frequency normalizations are applied simultaneously to all three components to preserve relative amplitude information. Cross-correlations are then computed for all station and

component pairs. Clear Rayleigh-wave moveout is observed in the 3–10 s period range in the ZZ, ZR, RZ, and RR components (Figure 2). The one-sided record section indicates that the dominant ambient noise energy originates from the ocean and propagates inland.

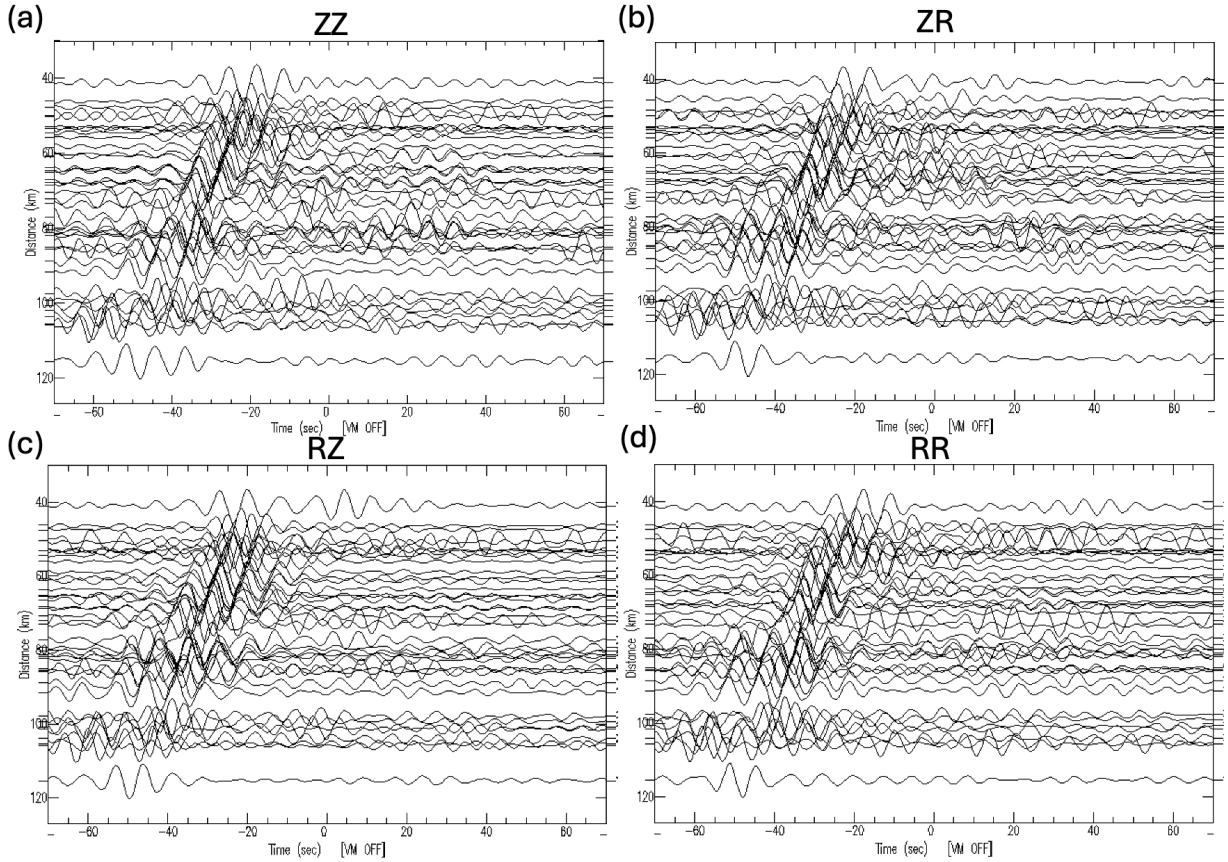

Figure 2. Example cross-correlation record section. (a) Vertical–vertical (ZZ) cross-correlations between BK station MTOS and all NP network stations bandpassed between 5-10 sec period. (b–d) Same as (a), but for vertical–radial (ZR), radial–vertical (RZ), and radial–radial (RR) cross-correlations.

For each station and period, we treat all other stations as sources and measure amplitude ratios between the ZZ and ZR and RZ and RR cross-correlations to obtain Rayleigh wave H/V ratios. Signal-to-noise ratio (SNR) and phase-shift criteria are applied to remove low-quality measurements. The phase-shift criterion ensures that the vertical and radial components exhibit the expected ~90° phase difference for Rayleigh waves. The final H/V ratios and their uncertainties are estimated from the mean and standard deviation of all accepted measurements.

Rayleigh Wave H/V Ratios and CMV Validation

Figure 3a and 3d summarize the observed H/V ratios at 4 and 6 s periods. Because H/V ratios are particularly sensitive to velocity contrasts in the shallow crust (Berg et al., 2018), high and low values are typically associated with sedimentary depocenters and mountainous regions, respectively. In our results, elevated H/V ratios are observed adjacent to the South Bay,

particularly in the Oakland and San Jose areas, consistent with the presence of shallow, low-velocity Quaternary sediments. Additional regions with high H/V ratios include areas near Monterey Bay, the California Delta/Central Valley, and the Livermore Basin (at 6 s). In contrast, near-unity H/V ratios (~1) are generally observed in surrounding mountainous/hill terrains.

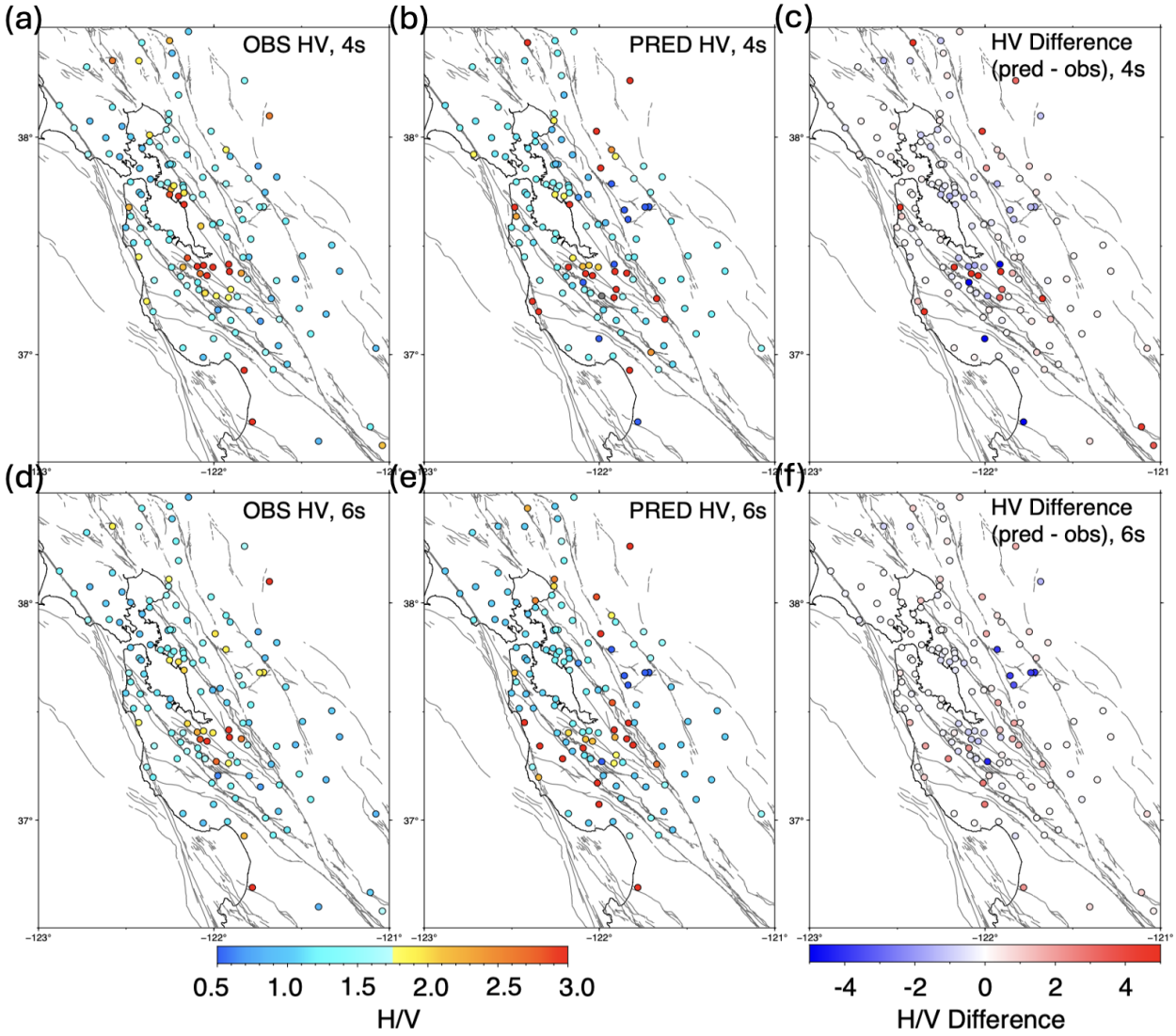

Figure 3. Observed and predicted Rayleigh-wave H/V ratios across the SFBA. (a) Observed H/V ratios at 4 s period. (b) Predicted 4 s H/V ratios based on the SFBA CVM. (c) Differences between predicted and observed 4 s H/V ratios, where blue and red indicate underestimation and overestimation of H/V ratios for CVM, respectively. (d–f) Same as (a–c), but for 6 s Rayleigh waves.

For each station, we compare the observed H/V ratios with predictions based on the SFBA CVM. We extract 1D velocity models from the 3D CVM and numerically compute the corresponding H/V ratios (Herrmann & Ammon, 2024). The predicted H/V ratios at 4 and 6 s periods, along with their differences from the observations, are summarized in Figures 3b–c and 3e–f. Overall, the predicted H/V ratios reproduce the main spatial patterns observed in the data, suggesting that the geology-based CVM captures the first-order features of the velocity

structure. However, several systematic discrepancies indicate that further refinement of the model is needed. In the Oakland region, observed H/V ratios are consistently higher than predictions, implying that the CVM underestimates the shallow velocity gradient. A similar pattern is observed near San Jose, although with greater spatial variability. In the Livermore Basin, predicted H/V ratios are also notably lower than observed values. As one of the deepest basins in the SFBA CVM, this discrepancy likely reflects an underestimation of the velocity gradient within the sedimentary layers. Station coverage in the Livermore Basin is relatively sparse, with most permanent stations located near the basin margins. Under a separate project funded by the USGS Earthquake Hazards Program, we recently deployed a dense geophone array in the Livermore Basin for two months. It is expected to significantly improve data coverage and help refine the model in this region.

1D inversions.

To demonstrate the potential of Rayleigh-wave H/V ratios for improving shallow crustal structure, we perform MCMC inversion (Shen et al., 2013) to jointly invert the observed H/V ratios and Rayleigh-wave phase velocities. To obtain location-dependent phase velocities, we first extract a 1D model at each station from the 3D model of Guo et al. (2025), which was constructed from joint surface-wave and body-wave travel-time tomography. This extracted 1D model is also used as the initial model for the MCMC inversion. We then compute the corresponding dispersion curve from the 1D model. These forward-calculated phase velocities are treated as observations, together with the measured H/V ratios, to invert for an updated 1D velocity model. Because phase velocities are generally sensitive to deeper structure than H/V ratios (Berg et al., 2018), the complementary sensitivities of the two datasets allow the crustal model to be constrained from shallow to greater depths.

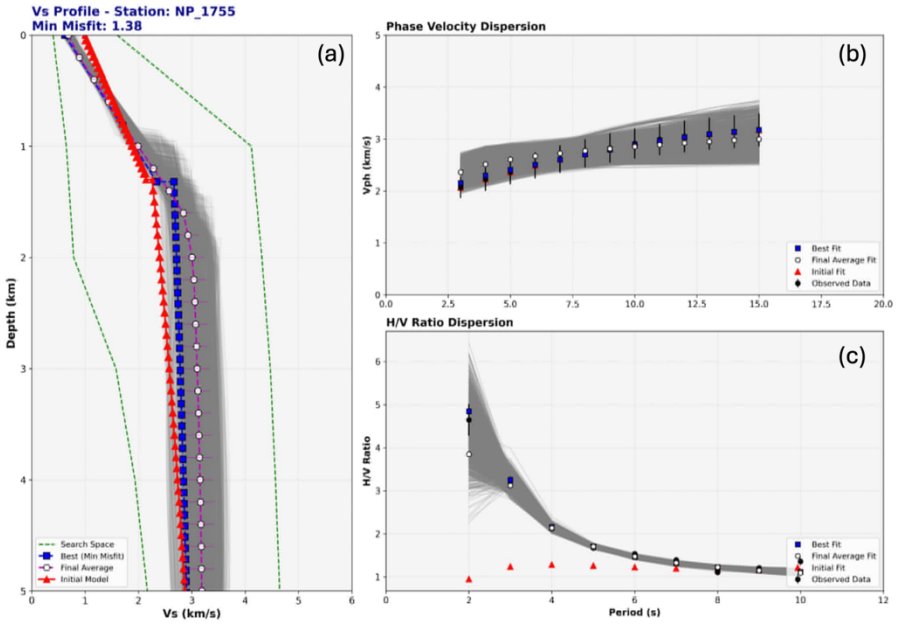

Figure 4. Example 1D MCMC inversion. (a) 1D Vs models at station 1755; red, gray, blue, and white curves denote the initial, acceptable, best-fit, and final (average) models, respectively. (b) Input and predicted phase velocities. (c) Observed and predicted Rayleigh-wave H/V ratios. Colors in (b) and (c) correspond to those in (a).

Figure 4a–c presents an example inversion for station 1755 (NP network) near Oakland. Significant discrepancies are evident between the observed H/V ratios and those predicted by the initial 1D model. In particular, the lower predicted H/V ratios at periods below 6 s indicate that the initial model underestimates the shallow velocity gradient. This is a common limitation of

travel-time-based tomography, on which our initial model is based, as it often lacks sensitivity to shallow structure and may smear deeper features into shallower depths due to regularization. Following MCMC inversion, the updated model exhibits a stronger shallow velocity gradient and produces H/V ratios that better match the observations while maintaining a good fit to the phase velocities. We apply this 1D MCMC inversion to all stations with available H/V measurements across the Bay Area.

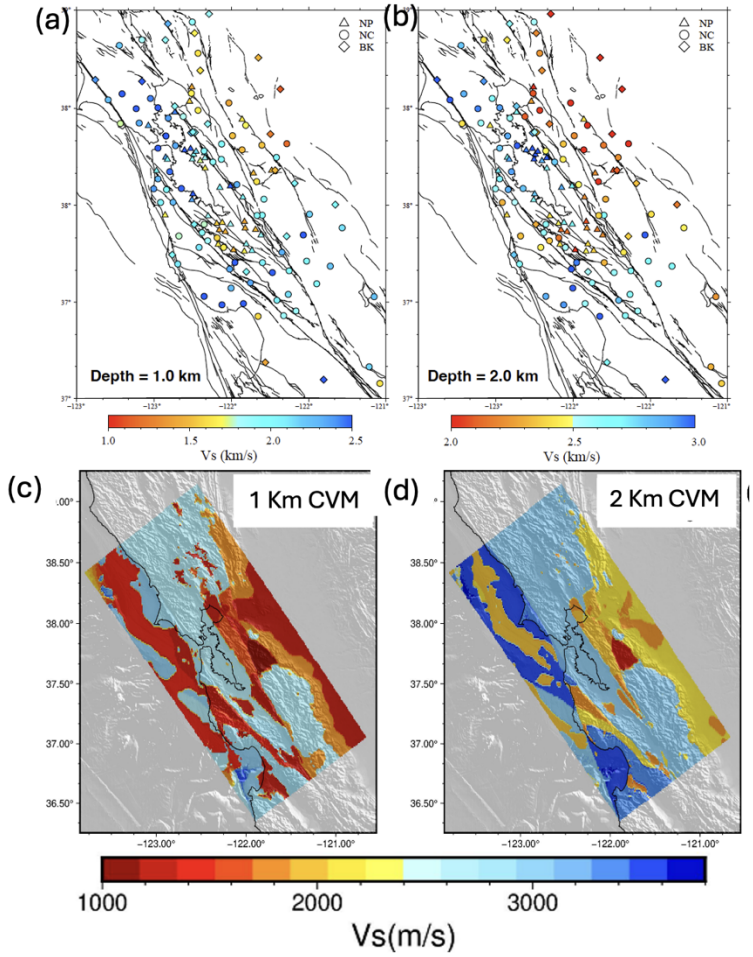

Figure 5. Comparison of inverted models and the CVM. (a–b) Inverted 1D Vs models at depths of 1 and 2 km; station symbols indicate the network (NP, NC, or BK). (c–d) SFBA CVM at depths of 1 and 2 km. Note that color scales differ between subplots.

Model Comparison

Shear-wave velocities at depths of 1 and 2 km derived from the MCMC inversion and the SFBA CVM are shown and compared in Figure 5. Overall, the major velocity structures are similar between the inverted models and the CVM and are consistent with surface geology. High velocities are observed in areas where the Franciscan Complex bedrock is exposed at the surface, whereas low velocities are found in regions underlain by Quaternary deposits. Despite these general similarities, notable differences exist in several areas. For example, low-velocity anomalies in the San Jose and Oakland regions adjacent to the South Bay appear to extend to greater depths in the inverted models, suggesting that the CVM may underestimate the depth to bedrock in these areas. Preliminary results from a separate project (SCEC Award 25296) suggest that incorporating our newly inverted 1D models can improve earthquake ground-motion predictions (see the associated project report).

Ongoing research

The initial phase of receiver functions is also sensitive to sedimentary structure and provides complementary constraints to surface-wave measurements, thereby enhancing resolution of the shallow crust (Kim et al., 2025). Processing of NC and BK stations has been completed, whereas processing of NP stations, which are critical for constraining structures near the Bay, is ongoing.

References

Aagaard, B.T., and Hirakawa, E.T. (2021). San Francisco Bay region 3D seismic velocity model v21.1. *U.S. Geological Survey data release*, https://doi.org/10.5066/P9TRDCHE.

Berg, E., F-C. Lin, A.A. Allam, H. Qiu, W. Shen, and Y. Ben-Zion. (2018). Tomography of Southern California via Bayesian Joint Inversion of Rayleigh Wave Ellipticity and Phase Velocity from Ambient Noise Cross-Correlations, Journal of Geophysical Research: Solid Earth, 123, 9933–9949. https://doi.org/10.1029/2018JB016269.

Herrmann, R. B., and C. J. Ammon (2004), Computer programs in seismology: Surface waves, receiver functions and crustal structure, manual, St. Louis Univ., St. Louis, Mo

Kim, H. J., Lin, F.-C., Pechmann, J. C., Hardwick, C. L., & McKean, A. P. (2025). Seismic imaging of the Salt Lake basin using joint inversion of receiver functions and Rayleigh wave data. Journal of Geophysical Research: Solid Earth, 130, e2024JB030927. https://doi.org/10.1029/2024JB030927

Lin, F.-C. and B. Schmandt. (2014). Upper crustal azimuthal anisotropy across the contiguous US determined by Rayleigh wave ellipticity, *Geophys. Res. Lett.*, 41, doi:10.1002/2014GL062362

Shen, W., Ritzwoller, M. H., Schulte-Pelkum, V., & Lin, F. C. (2013). Joint inversion of surface wave dispersion and receiver functions: a Bayesian Monte-Carlo approach. *Geophysical Journal International*, *192*(2), 807-836.